NOAA Technical Memorandum NWS NMC-59

DECOMPOSITION OF A WIND FIELD ON THE SPHERE

National Meteorological Center
Washington, D. C.
April 1976

noaa NATIONAL OCEANIC AND ATMOSPHERIC ADMINISTRATION / National Weather Service

er Series

The National Me
(NWS) produces weather anal-
yses and forecast
expanded to include the entire
globe. The Cente
cy of forecasts, to provide
information in the
as practicable.

NOAA Technical
ation of material of general
interest which
formally elsewhere at a later
date. Publication
Technical Notes (TN), Na-
tional Meterologi
gh 48 are in the former series
ESSA Technical Mem
inning with 49, publications
are now part of th

Publications lis
rmation Service (NTIS), U.S.
Department of Com
Va. 22151. Price: $3.00 paper
copy; $1.45 microfiche. Order
ssion number, when given, in parentheses.

Weather Bureau Technical Notes

TN 22 NMC 34 Tropospheric Heating and Cooling for Selected Days and Locations over the United States During Winter 1960 and Spring 1962. Philip F. Clapp and Francis J. Winninghoff, 1965. (PB-170-584)

TN 30 NMC 35 Saturation Thickness Tables for the Dry Adiabatic, Pseudo-adiabatic, and Standard Atmospheres. Jerrold A. LaRue and Russell J. Younkin, January 1966. (PB-169-382)

TN 37 NMC 36 Summary of Verification of Numerical Operational Tropical Cyclone Forecast Tracks for 1965. March 1966. (PB-170-410)

TN 40 NMC 37 Catalog of 5-Day Mean 700-mb. Height Anomaly Centers 1947-1963 and Suggested Applications. J. F. O'Connor, April 1966. (PB-170-376)

ESSA Technical Memoranda

WBTM NMC 38 A Summary of the First-Guess Fields Used for Operational Analyses. J. E. McDonell, February 1967. (AD-810-279)

WBTM NMC 39 Objective Numerical Prediction Out to Six Days Using the Primitive Equation Model--A Test Case. A. J. Wagner, May 1967. (PB-174-920)

WBTM NMC 40 A Snow Index. R. J. Younkin, June 1967. (PB-175-641)

WBTM NMC 41 Detailed Sounding Analysis and Computer Forecasts of the Lifted Index. John D. Stackpole, August 1967. (PB-175-928)

WBTM NMC 42 On Analysis and Initialization for the Primitive Forecast Equations. Takashi Nitta and John B. Hovermale, October 1967. (PB-176-510)

WBTM NMC 43 The Air Pollution Potential Forecast Program. John D. Stackpole, November 1967. (PB-176-949)

WBTM NMC 44 Northern Hemisphere Cloud Cover for Selected Late Fall Seasons Using TIROS Nephanalyses. Philip F. Clapp, December 1968. (PB-186-392)

WBTM NMC 45 On a Certain Type of Integration Error in Numerical Weather Prediction Models. Hans Okland, September 1969. (PB-187-795)

WBTM NMC 46 Noise Analysis of a Limited-Area Fine-Mesh Prediction Model. Joseph P. Gerrity, Jr., and Ronald D. McPherson, February 1970. (PB-191-188)

WBTM NMC 47 The National Air Pollution Potential Forecast Program. Edward Gross, May 1970. (PB-192-324)

WBTM NMC 48 Recent Studies of Computational Stability. Joseph P. Gerrity, Jr., and Ronald D. McPherson, May 1970. (PB-192-979)

(Continued on inside back cover)

NOAA Technical Memorandum NWS NMC-59

DECOMPOSITION OF A WIND FIELD ON THE SPHERE

Clifford H. Dey
John A. Brown, Jr.

National Meteorological Center
Washington, D. C.
April 1976

UNITED STATES
DEPARTMENT OF COMMERCE
Elliot L. Richardson, Secretary

NATIONAL OCEANIC AND
ATMOSPHERIC ADMINISTRATION
Robert M. White, Administrator

National Weather
Service
George P. Cressman, Director

CONTENTS

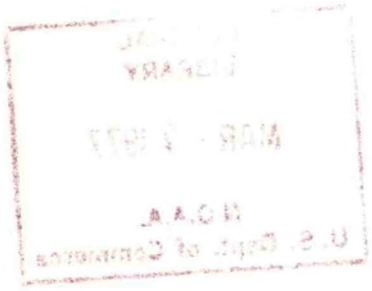

DECOMPOSITION OF A WIND FIELD ON THE SPHERE

by

Clifford H. Dey and John A. Brown, Jr.
National Meteorological Center
National Weather Service, NOAA, Washington, D.C.

ABSTRACT

When decomposing a horizontal wind field into its rotational and divergent components, care must be taken to assure compensating truncation errors in order that the resulting wind components can be used to accurately reconstruct the original field. An example is presented of a finite difference system with second-order accuracy for a regular spherical grid which yields results sufficiently accurate for use in initialization procedures for a primitive equation forecast model used at the National Meteorological Center (NMC).

1. Introduction

This paper is not presented to document a new idea in finite differencing, but rather to bring attention to a problem which is too often overlooked. When decomposing an atmospheric horizontal wind field at a particular vertical level into its rotational and divergent components, one should be careful to maintain a finite difference system which is internally consistent. By this we mean that the finite difference forms of the wind components and the vorticity and divergence should be established consistently from the stream function and velocity potential, both within the fluid and at the lateral boundaries.

In addressing the global forecast problem, personnel at the NMC have developed a grid point 8-layer global primitive equation model (Stackpole, Vanderman, and Shuman, 1973), hereafter referred to as the Global Model. Recent testing of this model has revealed the presence of large amplitude nonmeteorological oscillations in the forecast. In an attempt to reduce the portion of the noise due to initial mass-wind imbalances, it was necessary to develop a finite difference method for separating the analyzed wind (Flattery 1970) into its rotational and divergent components. The method presented here is an internally consistent finite difference system of second-order accuracy for a regular latitude-longitude grid. However, the general procedures of this method should be applicable to other systems as well.

In section 2, the accuracies of two finite difference systems are compared for a one-dimensional Cartesian grid. The details of the finite difference system for the spherical grid are presented in section 3. The lateral boundary conditions at the poles are considered in section 4. The numerical method for solving the problem is discussed in section 5. Finally, the results of testing the proposed technique on a real data case are presented in section 6.

2. Staggered and Nonstaggered Finite Difference Formulations

In one dimension, the relative vorticity (ξ) and the wind ($\hat{v}$) can be written as

$$\xi = \frac{\partial v}{\partial x} = \frac{\partial^2 \psi}{\partial x^2} \tag{1}$$

$$\hat{v} = \frac{\partial \psi}{\partial x} \tag{2}$$

where ψ represents the stream function. Consider the problem where the analyzed wind field (v) is given. Equation (1) will be used to obtain ψ and Equation (2) to calculate the reconstructed wind field $\hat{v}$. The finite difference forms of (1) and (2) should be consistent for the reconstructed wind field $\hat{v}$ to be equal to the original wind field v.

The first finite difference system we consider is one in which the vorticity ξ applies at the grid points where the analyzed winds are located. This will be termed the nonstaggered finite difference system. In this system, the finite difference forms of (1) and (2) are

$$\psi_{xx} = \overline{v}^{x}_{x} \tag{3}$$

$$\hat{v} = \overline{\psi}^{x}_{x} \tag{4}$$

in which the notations

$$(\,)_x = \frac{1}{\Delta x}\left[(\,)_{i+1} - (\,)_i\right]$$

$$\overline{(\,)}^{x} = \frac{1}{2}\left[(\,)_{i+1} + (\,)_i\right] \tag{5}$$

have been used. Here, Δx is the spatial grid distance. Thus at point i, Equations (3) and (4) are, respectively,

$$\frac{1}{(\Delta x)^2}\left[\psi_{i+1} + \psi_{i-1} - 2\psi_i\right] = \frac{1}{2\Delta x}\left[v_{i+1} - v_{i-1}\right] \tag{6}$$

and

$$\hat{v}_i = \frac{1}{2\Delta x}[\psi_{i+1} - \psi_{i-1}]. \tag{7}$$

Assume solutions for the analyzed wind and the stream function are given by

$$v_i = A \sin\left[\frac{2\pi i}{L}\right] \tag{8}$$

$$\psi_i = B \cos\left[\frac{2\pi i}{L}\right] \tag{9}$$

where $L\Delta x$ is the wavelength. Substituting (8) and (9) into (6) yields

$$\psi_i = \frac{A\Delta x}{2} \cos\left[\frac{2\pi i}{L}\right]\left\{ \frac{\sin\left[\frac{2\pi}{L}\right]}{\cos\left[\frac{2\pi}{L}\right] - 1} \right\}. \tag{10}$$

Substituting this into (7) finally gives

$$\hat{v}_i = v_i \cos^2\left[\frac{\pi}{L}\right]. \tag{11}$$

Equation (11) shows that the reconstructed wind field $\hat{v}_i$ will underestimate the analyzed wind field v_i due to noncompensating truncation errors.

A finite difference system containing noncompensating truncation errors was used by Washington and Baumhefner (1974) in their search for a suitable global initialization scheme. After setting the vertically integrated mass-divergence to zero everywhere, their reconstructed wind fields had the same patterns as the original fields but the magnitudes of the reconstructed fields were up to 13 m sec^{-1} smaller than those of the original. The largest decreases were in the vicinity of the jet maxima.

Let us now consider the second finite difference formulation in which the vorticity applies between the grid points where the winds are located. This will be referred to as the staggered system. In this case, the differential equations (1) and (2) are approximated by

$$\xi = v_x = \psi_{xx} \tag{12}$$

and

$$\hat{v} = \psi_x \,. \tag{13}$$

When $\hat{v}$ in (13) is substituted for v in (12), a perfect equality is obtained. Thus, truncation error will be perfectly compensated in the staggered system.

A staggered finite difference system for decomposing global horizontal wind analyses is presented in the next section.

3. A Staggered Finite Difference Formulation of the Spherical Problem

The decomposition of a horizontal wind field into its rotational and divergent components is accomplished by solving the equations

$$\vec{\nabla} \cdot \vec{\nabla}\psi = \xi \tag{14}$$

and

$$\vec{\nabla} \cdot \vec{\nabla}\chi = D, \tag{15}$$

in which ξ is the relative vorticity, D is the divergence, ψ is the stream function, χ is the velocity potential, and $\vec{\nabla}$ is the horizontal gradient operator. The reconstruction of a wind field from such components is accomplished via Helmholtz' theorem

$$\vec{\nabla} = \vec{k} \times \vec{\nabla}\psi + \vec{\nabla}\chi, \tag{16}$$

where $\vec{\nabla}$ is the reconstructed wind field.

In spherical horizontal coordinates (ϕ = latitude, λ = longitude), equations (14) and (15) can be written as, respectively,

$$\frac{\partial}{\partial\lambda}\left[\frac{1}{\cos\phi}\frac{\partial\psi}{\partial\lambda}\right] + \frac{\partial}{\partial\phi}\left[\cos\phi\frac{\partial\psi}{\partial\phi}\right] = \frac{\partial}{\partial\lambda}[rv] - \frac{\partial}{\partial\phi}[ru\cos\phi] \tag{17}$$

$$\frac{\partial}{\partial\lambda}\left[\frac{1}{\cos\phi}\frac{\partial\chi}{\partial\lambda}\right] + \frac{\partial}{\partial\phi}\left[\cos\phi\frac{\partial\chi}{\partial\phi}\right] = \frac{\partial}{\partial\lambda}[ru] + \frac{\partial}{\partial\phi}[rv\cos\phi]. \tag{18}$$

In these equations, u and v are winds from the west and south, respectively, r is the radius of the earth,

$$-\frac{\pi}{2} \le \phi \le \frac{\pi}{2}, \quad \text{and } 0 \le \lambda \le 2\pi .$$

Both sides of (17) and (18) have been multiplied by $[r^2\cos\phi]$. Likewise, the wind components defined by (16) can be written in spherical coordinates as

$$u = -\frac{1}{r}\frac{\partial\psi}{\partial\phi} + \frac{1}{r\cos\phi}\frac{\partial\chi}{\partial\lambda}\,, \tag{19}$$

$$v = \frac{1}{r\cos\phi}\frac{\partial\psi}{\partial\lambda} + \frac{1}{r}\frac{\partial\chi}{\partial\phi}\,. \tag{20}$$

The staggered finite difference formulations of equations (17) through (20) are:

$$\overline{\left[\frac{1}{\cos\phi}\,\overline{\psi}^{\phi}_{\lambda}\right]}^{\phi}_{\lambda} + \overline{\left[\cos\phi\,\overline{\psi}^{\lambda}_{\phi}\right]}^{\lambda}_{\phi} = r\,\overline{v}^{\phi}_{\lambda} - \overline{[u\cos\phi]}^{\lambda}_{\phi}\,, \tag{21}$$

$$\overline{\left[\frac{1}{\cos\phi}\,\overline{\chi}^{\phi}_{\lambda}\right]}^{\phi}_{\lambda} + \overline{\left[\cos\phi\,\overline{\chi}^{\lambda}_{\phi}\right]}^{\lambda}_{\phi} = r\,\overline{u}^{\phi}_{\lambda} + \overline{[v\cos\phi]}^{\lambda}_{\phi}\,, \tag{22}$$

$$u = -\frac{1}{r}\,\overline{\psi}^{\lambda}_{\phi} + \frac{1}{r\cos\phi}\,\overline{\chi}^{\phi}_{\lambda}\,, \tag{23}$$

$$v = \frac{1}{r\cos\phi}\,\overline{\psi}^{\phi}_{\lambda} + \frac{1}{r}\,\overline{\chi}^{\lambda}_{\phi}\,. \tag{24}$$

The grid arrangement and location of variables is shown in Figure 1. The finite differences symbolized in equations (21)-(24) have the following meanings:

$$\left[\overline{(\,)}^{\phi}_{\lambda}\right]_{i+\frac{1}{2},j+\frac{1}{2}} = \frac{1}{2\Delta\lambda}\left[(\,)_{i+1,j+1} - (\,)_{i,j+1} + (\,)_{i+1,j} - (\,)_{i,j}\right], \tag{25}$$

$$\left[\overline{(\,)}^{\lambda}_{\phi}\right]_{i+\frac{1}{2},j+\frac{1}{2}} = \frac{1}{2\Delta\phi}\left[(\,)_{i+1,j+1} - (\,)_{i+1,j} + (\,)_{i,j+1} - (\,)_{i,j}\right], \tag{26}$$

$$\begin{aligned}\left(\overline{\left[\frac{1}{\cos\phi}\,\overline{(\,)}^{\phi}_{\lambda}\right]}^{\phi}_{\lambda}\right)_{i,j} = \frac{1}{4(\Delta\lambda)^2}\Bigg\{ & \frac{1}{\cos\phi_{j+\frac{1}{2}}}\left[(\,)_{i+1,j+1} - 2(\,)_{i,j+1} + (\,)_{i-1,j+1}\right.\\ & \left. + (\,)_{i+1,j} - 2(\,)_{i,j} + (\,)_{i-1,j}\right]\\ & + \frac{1}{\cos\phi_{j-\frac{1}{2}}}\left[(\,)_{i+1,j} - 2(\,)_{i,j} + (\,)_{i-1,j}\right.\\ & \left. + (\,)_{i+1,j-1} - 2(\,)_{i,j-1} + (\,)_{i-1,j-1}\right]\Bigg\}\,,\end{aligned} \tag{27}$$

$$\left(\overline{\overline{[\cos\phi(\ )^{\lambda}]_{\phi}}^{\lambda}}\right)_{i,j} = \frac{1}{4(\Delta\phi)^2}\{\cos\phi_{j+\frac{1}{2}}[(\ )_{i+1,j+1} + 2(\ )_{i,j+1}$$

$$+ (\ )_{i-1,j+1} - (\ )_{i+1,j} - 2(\ )_{i,j} - (\ )_{i-1,j}]$$

$$- \cos\phi_{j-\frac{1}{2}}[(\ )_{i+1,j} + 2(\ )_{i,j} + (\ )_{i-1,j}$$

$$- (\ )_{i+1,j-1} - 2(\ )_{i,j-1} - (\ )_{i-1,j-1}]\} \ . \qquad (28)$$

Here, $\Delta\phi = \Delta\lambda$, the grid point separation distance in radians. Equations (21) and (22) are solved by the accelerated Liebmann relaxation scheme, and a wind field can be reconstructed via equations (23) and (24). The relations in this section are valid everywhere except at the poles. There suitable boundary conditions must be used.

4. Boundary Conditions at the Poles

At the North and South Poles, the grid arrangement is different from that in the rest of the grid. This is shown in Figure 2 for the North Pole. An assumption about the wind at the poles was made in order to obtain finite difference representations of equations (14) and (15) at point 5 in Figure 2. The assumption is identified and the resulting finite difference equations are presented in this section.

Let circulation (C) be defined as

$$C = \oint \vec{V} \cdot d\vec{s} \qquad (29)$$

and vorticity by

$$\xi = [C/\Delta A] = [1/\Delta A] \oint \vec{V} \cdot d\vec{s} \ , \qquad (30)$$

where ΔA is the area enclosed by the circulation and $\vec{s}$ is a unit vector tangent to the line enclosing ΔA. In a similar manner, let divergence be defined by

$$D = [1/\Delta A] \oint \vec{V} \cdot d\vec{n} \ , \qquad (31)$$

in which $\vec{n}$ is a unit outward vector normal to the line enclosing ΔA. The convention used here is that positive ξ is counterclockwise circulation and positive D is net outflow. Equations (30) and (31) are approximated for the area bounded by points a, b, and c in Figure 2 as follows:

$$\xi = \frac{1}{\Delta A}\{h_1\left[\frac{-v_a - v_b}{2}\right] + h_2\left[\frac{u_b + u_c}{2}\right] + h_3\left[\frac{v_c + v_d}{2}\right]\} \ , \qquad (32)$$

$$D = \frac{1}{\Delta A}\{h_1[\frac{-u_a-u_b}{2}] + h_2[\frac{-v_b-v_c}{2}] + h_3[\frac{u_c+u_d}{2}]\} . \tag{33}$$

The quantities h_1, h_2, h_3, and ΔA are given by

$$\begin{aligned} h_1 &= h_3 = r\Delta\phi , \\ h_2 &= r\Delta\lambda \cos\phi_{bc} , \\ \Delta A &= r^2\Delta\lambda[1 - \sin\phi_{bc}] . \end{aligned} \tag{34}$$

It will be useful to express ΔA as

$$\Delta A = r^2\Delta\lambda\Delta\phi \cos\phi_o . \tag{35}$$

For this to be true,

$$\Delta\phi \cos\phi_o = 1 - \sin\phi_{bc} ,$$

so that ϕ_o is defined by

$$\phi_o = \cos^{-1}[\frac{1 - \sin\phi_{bc}}{\Delta\phi}] . \tag{36}$$

Substitution of (34) and (35) into (32) and (33) changes the latter into, respectively,

$$\xi = \frac{1}{r^2\cos\phi_o}\{\frac{r}{2\Delta\lambda}[v_d-v_a] + \xi'\} , \tag{37}$$

$$D = \frac{1}{r^2\cos\phi_o}\{\frac{r}{2\Delta\lambda}[u_d-u_a] + D'\} , \tag{38}$$

in which ξ' and D' are given by

$$\xi' = \frac{r}{2\Delta\lambda}[v_c-v_b] + \frac{r\cos\phi_{bc}}{2\Delta\phi}[u_b+u_c] , \tag{39}$$

$$D' = \frac{r}{2\Delta\lambda}[u_c-u_b] + \frac{r\cos\phi_{bc}}{2\Delta\phi}[-v_b-v_c] . \tag{40}$$

The winds at points b and c are defined in terms of ψ and χ just as in the previous section. The boundary condition lies in the specification

of the winds at the pole (point a). The NMC Global Model carries one vector wind at the pole and resolves that wind into u and v components at each longitude where gridpoints lie. In practice, therefore, u_d and v_d do not differ greatly from u_a and v_a respectively. Because of this, we assumed

$$u_a = u_d \quad \text{and} \quad v_a = v_d \, . \tag{41}$$

This reduces (37) and (38) to

$$\xi = \xi'/r^2\cos\phi_o \tag{42}$$

$$D = D'/r^2\cos\phi_o \tag{43}$$

Substitution of the finite difference representations for u and v at points b and c given in the previous section transforms (39) and (40) into (after multiplying through by $r^2\cos\phi_o$)

$$\xi' = \overset{*}{\nabla}^2\psi - R(\chi), \tag{44}$$

$$D' = \overset{*}{\nabla}^2\chi + R(\psi), \tag{45}$$

where

$$\begin{aligned}\overset{*}{\nabla}^2 = \frac{1}{2\Delta\lambda}\Big\{\frac{1}{2\Delta\lambda\,\cos\phi_{bc}}\big[(\,)_4 - 2(\,)_5 + (\,)_6 + (\,)_7 \\ - 2(\,)_8 + (\,)_9\big]\Big\} + \frac{1}{2\Delta\phi}\Big\{\frac{\cos\phi_{bc}}{2\Delta\phi}\big[-(\,)_4 \\ - 2(\,)_5 - (\,)_6 + (\,)_7 + 2(\,)_8 + (\,)_9\big]\Big\} \, ,\end{aligned} \tag{46}$$

$$R(\,) = \frac{1}{4\Delta\phi\Delta\lambda}\big[-2(\,)_4 + 2(\,)_6\big] \, . \tag{47}$$

5. Solution of the Finite Difference Equations

The complete system consists of equations (21) and (22) at all interior gridpoints, equations (44) and (45) at the row of gridpoints nearest the North Pole (87.5°N for a 5° latitude-longitude grid), and equations similar to (44) and (45) at the row of gridpoints nearest the South Pole (87.5°S for a 5° latitude-longitude grid). The wind field

was reconstructed from ψ and χ fields via equations (23) and (24) for all gridpoints except at the poles. There, the averaging procedure used in the Global Model was invoked.

The consequences of equations (44) and (45) are that the solution for ψ depends on the values of χ at 87.5°N and S latitude, and the solution for χ depends on the values of ψ at 87.5°N and S latitude (again for a 5° grid). Thus, a special procedure was necessary to solve for ψ and χ.

The scheme used was to make an initial guess of $R(\chi) = 0$ at the northern and southernmost rows of gridpoints and solve for ψ by relaxation. Having ψ, $R(\psi)$ was computed at the row of gridpoints nearest each pole and a solution for χ was obtained by relaxation. Although this procedure could be iterated, it was found that additional cycles added little to the accuracy of the reconstructed winds.

6. Accuracy of the Solution

In order to test the accuracy of the method just described, a simple numerical experiment was devised. First, an analyzed wind field was produced by the global spectral analysis technique of Flattery (1970) on a 5° latitude-longitude grid. Then this analyzed wind field was decomposed into a stream function and a velocity potential, from which a second wind field was constructed via Helmholtz' Theorem. The quality of the solution method was judged on the basis of root-mean-square (RMS) differences between the original and reconstructed wind fields.

The results of the experiment, presented in Table 1, indicate that the reconstructed wind field is nearly identical to the original, the RMS differences being of the order of 0.01 m sec^{-1}. The effect of the boundary condition can be seen in the tendency for the RMS differences to increase towards the poles. However, even there the largest individual differences were only 0.05 m sec^{-1}. On the basis of these results, the solution method is considered to be adequate for use in initialization procedures for the Global Model.

7. Summary and Conclusions

The necessity of using an internally consistent finite difference formulation to decompose a horizontal wind field into its rotational and divergent components in order that these components can be used to accurately reconstruct the original field is demonstrated. Such an internally consistent finite difference system is developed to decompose a global wind field into a stream function and a velocity potential and reconstruct a global wind field from the components. The method requires a boundary condition at the poles. The procedure is found to be

Table 1. RMS[Original $(u,v,|\vec{v}|$ - Reconstructed $(u,v,|\vec{v}|)$] (in m sec^{-1})

Latitude	RMS u Difference	RMS v Difference	RMS $\|\vec{v}\|$ Difference
90°N	0.0011	0.0011	0.0008
85°N	0.0245	0.0233	0.0245
80°N	0.0177	0.0183	0.0206
75°N	0.0162	0.0158	0.0172
70°N	0.0141	0.0140	0.0127
65°N	0.0121	0.0124	0.0130
60°N	0.0107	0.0112	0.0105
55°N	0.0095	0.0100	0.0093
50°N	0.0084	0.0092	0.0092
45°N	0.0077	0.0084	0.0066
40°N	0.0071	0.0079	0.0070
35°N	0.0065	0.0074	0.0070
30°N	0.0061	0.0070	0.0061
25°N	0.0057	0.0067	0.0054
20°N	0.0054	0.0066	0.0054
15°N	0.0052	0.0064	0.0055
10°N	0.0049	0.0065	0.0059
5°N	0.0048	0.0064	0.0047
0°	0.0047	0.0066	0.0056
5°S	0.0047	0.0067	0.0054
10°S	0.0047	0.0069	0.0061
15°S	0.0049	0.0070	0.0053
20°S	0.0049	0.0073	0.0057
25°S	0.0051	0.0075	0.0057
30°S	0.0051	0.0079	0.0057
35°S	0.0056	0.0081	0.0061
40°S	0.0057	0.0085	0.0062
45°S	0.0062	0.0088	0.0069
50°S	0.0067	0.0094	0.0072
55°S	0.0077	0.0100	0.0081
60°S	0.0088	0.0109	0.0086
65°S	0.0103	0.0118	0.0103
70°S	0.0123	0.0133	0.0121
75°S	0.0169	0.0151	0.0150
80°S	0.0222	0.0183	0.0198
85°S	0.0242	0.0198	0.0211
90°S	0.0003	0.0003	0.0002

RMS u Difference (whole grid) 0.0106

RMS v Difference (whole grid) 0.0109

RMS $|\vec{v}|$ Difference (whole grid) 0.0105

sufficiently accurate for use in initialization experiments with the NMC eight-layer global model. However, it should be possible to use this solution method in conjunction with other numerical models as well by following the general procedure outlined here and tailoring the details to the model in question.

Acknowledgment

The authors wish to thank Ronald D. McPherson for many useful discussions.

References

Flattery, T. W., 1970: "Spectral Models for Global Analysis and Forecasting," Proceedings of the Sixth AWS Technical Exchange Conference, U.S. Naval Academy, September 21-24, 1970, Air Weather Service Technical Report 242.

Stackpole, J. D., Vanderman, L. W., and Shuman, F. G., 1974: "The NMC 8-layer Global Primitive Equation Model on a Latitude-Longitude Grid," Modelling for the First GARP Global Experiment, GARP Publication Series No. 14, June 1974, pp. 79-93.

Washington, W. M., and Baumhefner, D. P., 1974: "A Method of Removing Lamb Waves from Initial Data for Primitive Equation Models," Journal of Applied Meteorology, Vol. 14, No. 1, February 1975, pp. 114-119.

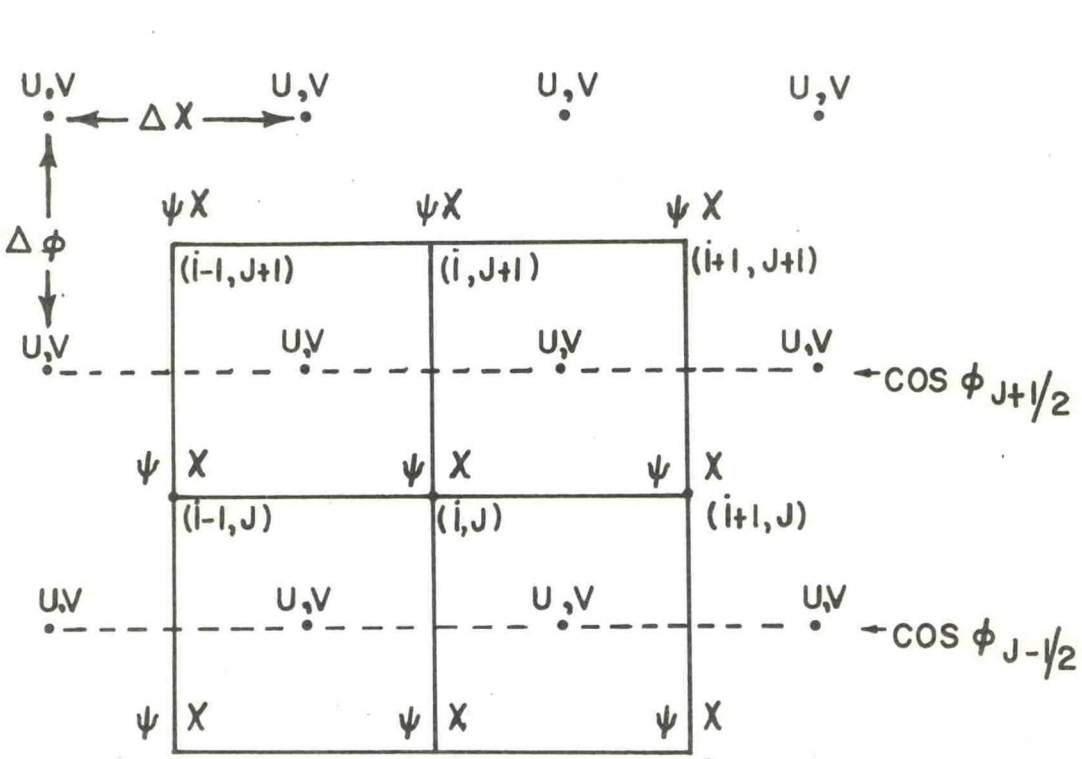

Figure 1. Grid arrangement and location of variables in the interior of the grid.

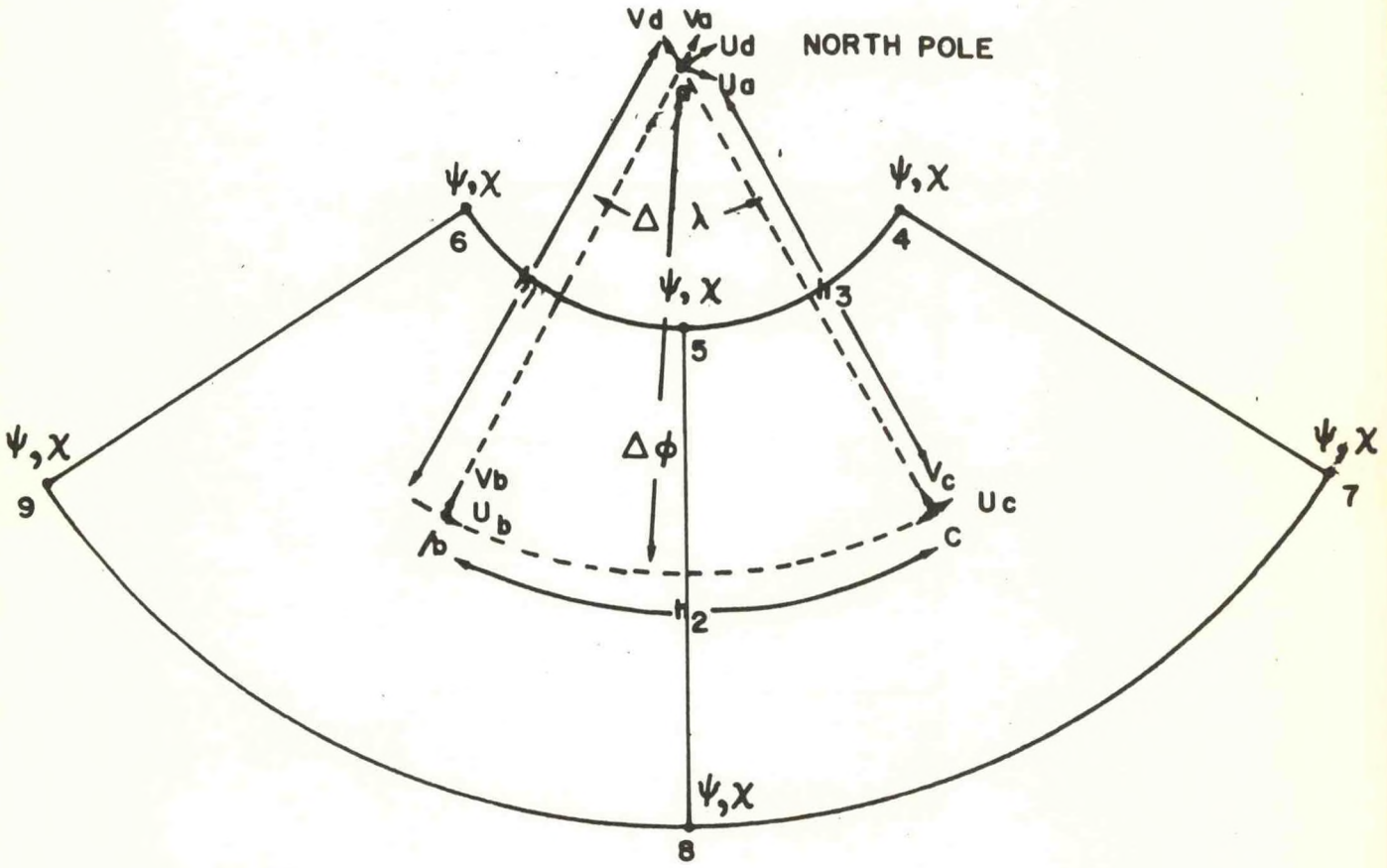

Figure 2. Grid arrangement and location of variables at the North Pole.

(Continued from inside front cover)

NOAA Technical Memoranda

NWS NMC 49 A Study of Non-Linear Computational Instability for a Two-Dimensional Model. Paul D. Polger, February 1971. (COM-71-00246)

NWS NMC 50 Recent Research in Numerical Methods at the National Meteorological Center. Ronald D. McPherson, April 1971.

NWS NMC 51 Updating Asynoptic Data for Use in Objective Analysis. Armand J. Desmarais, December 1972. (COM-73-10078)

NWS NMC 52 Toward Developing a Quality Control System for Rawinsonde Reports. Frederick G. Finger and Arthur R. Thomas, February 1973. (COM-73-10673)

NWS NMC 53 A Semi-Implicit Version of the Shuman-Hovermale Model. Joseph P. Gerrity, Jr., Ronald D. McPherson, and Stephen Scolnik. July 1973. (COM-73-11323)

NWS NMC 54 Status Report on a Semi-Implicit Version of the Shuman-Hovermale Model. Kenneth Campana, March 1974. (COM-74-11096/AS)

NWS NMC 55 An Evaluation of the National Meteorological Center's Experimental Boundary Layer model. Paul D. Polger, December 1974. (COM-75-10267/AS)

NWS NMC 56 Theoretical and Experimental Comparison of Selected Time Integration Methods Applied to Four-Dimensional Data Assimilation. Ronald D. McPherson and Robert E. Kistler, April 1975. (COM-75-10882/AS)

NWS NMC 57 A Test of the Impact of NOAA-2 VTPR Soundings on Operational Analyses and Forecasts. William D. Bonner, Paul L. Lemar, Robert J. Van Haaren, Armand J. Desmarais, and Hugh M. O'Neil, February 1976. (PB-256075)

NWS NMC 58 Operational-Type Analyses Derived Without Radiosonde Data from NIMBUS 5 and NOAA 2 Temperature Soundings. William D. Bonner, Robert van Haaren, and Christopher M. Hayden, March 1976. (PB-256099)